DOI: 10.1002/ejic.200700669

A Triphenylamine/Bis(terpyridine)Ir^{III} Dyad for the Assembly of Charge-Separation Constructs with Improved Performances

Lucia Flamigni,*[a] Barbara Ventura,[a] Etienne Baranoff,[b] Jean-Paul Collin,*[b] and Jean-Pierre Sauvage*[b]

Keywords: Charge separation / Electron transfer / Iridium / Photochemistry / Supramolecular chemistry

A new dyad **DII-Ir** consisting of a triphenylamine donor and a bis(terpyridine)Ir^{III} acceptor separated by a bridge composed of two benzamide groups has been synthesized. The electrochemical and photophysical properties of the dyad have been compared to those of a corresponding dyad **D-Ir** characterized by a bridge connecting the donor and the acceptor consisting of a single benzamide unit. We show that, whereas the charge-separation steps are still very efficient in the long dyad (≥99 %), charge recombination is slowed by a factor of three with respect to the short dyad. This encourages the use of this dyad in the assembly of a more elaborate array DII-Ir-A, expected to overcome the disappointingly low charge-separation yield of a previously studied **D-Ir-A** short triad.

Introduction

The process of producing long-lived charge-separated (CS) states is the basic event in artificial photosynthesis, which aims at efficiently converting light into chemical energy. In spite of the impressive results achieved in the last decade in multi-component arrays,[1] genuine long-lived CS states are still a valuable goal, especially when they involve less common or unexplored chromophores with respect to more conventional tetrapyrrolic or fullerene derivatives.[2] The most convenient and better tested strategy for producing genuine and indisputable CS states is that of using weakly coupled multi-component structures and of moving the electron, through a sequence of electron-transfer events, to molecular components far away from the hole. The first electron-transfer step is driven by light, whereas the following ones are ground-state electron-transfer reactions. A few years ago we started to use (terpyridine-type)Ir^{III} complexes as functional assembling units of multi-component structures having either the role of electron relay[2d,3] or of photosensitizer.[4] The use of this type of complexes proved to be very valuable both for the high energy level (ca. 2.5 eV) of its excited state, a ligand-centered triplet (^{3}LC) occasionally with some charge-transfer triplet (^{3}CT) character, and for the relative ease of reduction, –0.75 V vs. SCE.[5] The high excited-state energy level prevented draining of the electronic energy of the other components due to energy transfer, and the relative ease of reduction of the complex unit provided a high driving force for the primary photoinduced electron transfer starting the sequence. By using arrays with a central bis(terpyridine)Ir^{III} complex and appended porphyrins with suitable metallation to provide a good electron donor [free-base or (porphyrin)zinc complex] or a good electron acceptor [(porphyrin)gold(III) complex], respectively, we succeeded in producing a CS state with a lifetime of 450 ns and 100% yield.[2d,6]

More recently, we studied a **D-Ir-A** triad, where D is a triphenylamine electron donor, A is a naphthalenebis(imide) electron acceptor, and Ir is a bis(terpyridine)Ir^{III} complex (Scheme 1).

The lifetime of the CS state with opposite charges localized at the extremities of the array, produced upon light absorption by either the D or Ir unit is remarkable, of the order of 120 μs at ambient temperature in air-free acetonitrile (100 μs in air-saturated samples), but the yield of charge separation is quite modest, of the order of 10%.[7] The reason for this inefficiency is that the intermediate CS state D^+-Ir$^-$-A, formed with a 100% yield by a primary electron-transfer step originating from either an excited D unit (^{1}D) or excited Ir unit (^{3}Ir), can deactivate to the ground state faster ($k = 1.4 \times 10^{10}$ s^{-1}) than the rate at which it undergoes a further electron-transfer step ($k = 2.4 \times 10^9$ s^{-1}) leading to the final CS state D^+-Ir-A$^-$. We reasoned that increasing the D to Ir separation from ca. 1.6 nm in the original system to a distance of ca. 2.3 nm by inserting a further benzamide linker as in **DII-Ir** (Scheme 2), could be a possible strategy to improve the final CS yield in a triad DII-Ir-A.

[a] Istituto ISOF-CNR,
Via P. Gobetti 101, 40129 Bologna, Italy
E-mail: flamigni@isof.cnr.it
[b] Laboratoire de Chimie Organo-Minérale, UMR 7177 CNRS, Université Louis Pasteur,
Institut Le Bel, 4, rue Blaise Pascal, 67070 Strasbourg, France
E-mail: jpcollin@chimie.u-strasbg.fr
sauvage@chimie.u-strasbg.fr

Supporting information for this article is available on the WWW under http://www.eurjic.org or from the author.

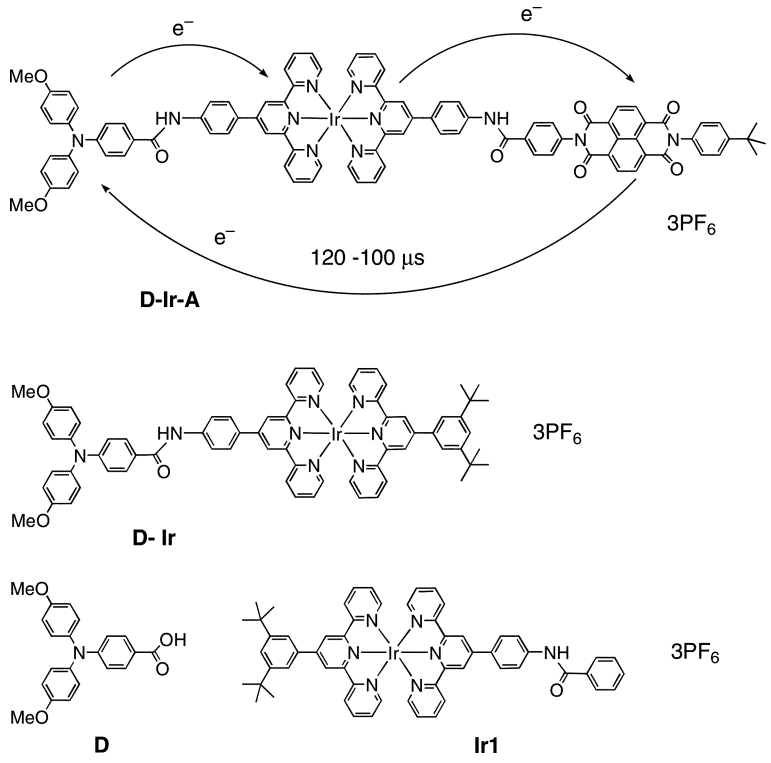

Scheme 1. Structures of the previously reported triad **D-Ir-A** and related models.

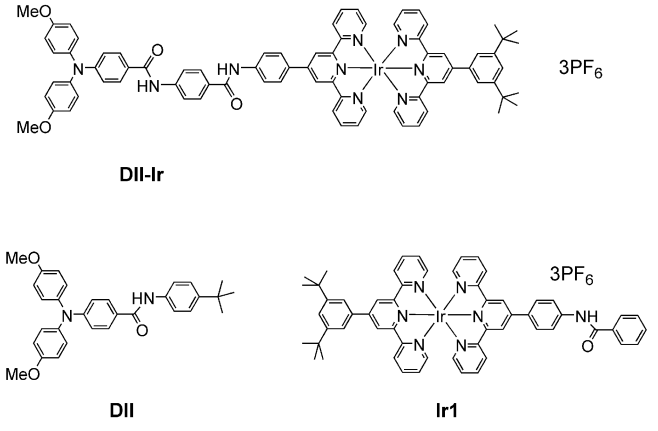

Scheme 2. Structures of the dyad **DII-Ir** and models reported in this work.

Decrease of both charge-separation (^{1}DII-Ir or DII-^{3}Ir $\rightarrow$ DII$^+$-Ir$^-$) and charge-recombination (DII$^+$-Ir$^-$ $\rightarrow$ D-Ir) rates are expected after increasing the D–Ir distance but, whereas a slight decrease in the 100% efficiency of the charge separation step can be afforded without being too detrimental to the overall CS process, a decrease in the rate of charge recombination in the dyad **DII-Ir** can have important effects on the overall charge separation over the extreme components in the derived triad DII-Ir-A. Since the synthesis of the latter requires a significant synthetic effort, we decided to verify first if the properties of the component dyad could suggest better performances for the derived triad, before undertaking the demanding synthesis of the more complex array. Therefore, the present report deals with the synthesis and photophysical properties of the dyad **DII-Ir** in order to evaluate its suitability for the construction of a triad DII-Ir-A with improved properties with respect to **D-Ir-A**.

Results and Discussion

The systems studied in this work are the dyad **DII-Ir** and the pertinent models **DII** and **Ir1**, reported in Scheme 2. Whereas complex **Ir1** had been previously examined and its properties will be only briefly summarized, **DII** and **DII-Ir** will here be examined in detail, and their properties will be compared with those of the short counterparts **D** and **D-Ir** previously reported.[7,8] In the following discussion the terms Ir and DII (not bold) will be used to indicate the Ir metal complex (with model **Ir1**) and the donor units (with model **DII**), respectively, within the dyad.

Synthesis

The dyad **DII-Ir** has been prepared according to the reactions shown in Scheme 3. The terpyridine **2** was prepared in two steps by homologation of the already known 4′-(4-aminophenyl)-2,2′:6′,2′′-terpyridine[9] with 4-nitrobenzoyl chloride and then by reduction of the nitro group with hydrazine in the presence of a catalytic amount of palladium on charcoal. The terpyridine **3**, bearing a triarylamine donor group linked to the terpy fragment by two amide brid-

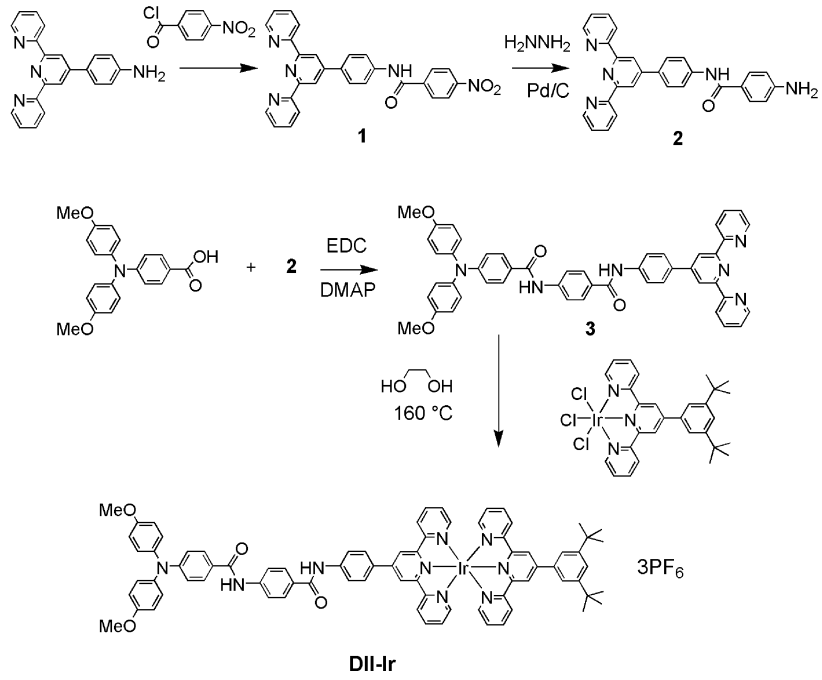

Scheme 3. Synthesis of the dyad **DII-Ir**.

ges, was prepared by condensation of the terpyridine **2** with 4-[bis(4-methoxyphenyl)amino]benzoic acid, in the presence of DMAP and EDC (peptidic coupling).[10] The dyad **DII-Ir** was obtained in 70% yield by reaction of the precursor [4′-(3,5-di-*tert*-butylphenyl)-2,2′:6′,2′′-terpyridine]-$IrCl_3$[5a] with the terpyridine **3** in ethylene glycol at 160 °C during 20 min.

Electrochemistry

The redox characteristics of the reference compounds **Ir1** and **DII** as well as that of the dyad **DII-Ir** examined by cyclic voltammetry in CH_3CN are reported with the values previously obtained for **D** and **D-Ir** in Table 1. One-electron reversible waves were observed for all the redox processes, in the dyad they were easily assigned to the corresponding individual components. A few mV of difference with respect to the short dyad **D-Ir** are observed in the redox couples of the donor group (D^+/D) and of the complex (terpy/terpy$^-$). Clearly, the presence of a second amide bridge in the dyad **DII-Ir** weakens even more the electronic coupling between the two redox entities.

Table 1. Cyclic voltammetry data of the reference compounds **Ir1**, **DII,** and the dyad **DII-Ir** in acetonitrile, 0.1 M nBu_4NPF_6, with SCE as a reference. Values for dyad **D-Ir** and model **D** are also reported.[7]

	$E_{1/2}$ (V vs. SCE)	
	D^+/D	terpy/terpy$^-$
Ir1		–0.76
D	0.80	
D-Ir	0.75	–0.75
DII	0.76	
DII-Ir	0.76	–0.78

Absorption Spectroscopy

The absorption spectra in acetonitrile of the components, their superposition, and the experimental spectrum of the array are reported in Figure 1. There is, within experimental errors, a good overlap of the experimental spectrum of **DII-Ir** with the calculated superposition of the model components in the 250–350 nm range, whereas the array spectrum differs slightly from the calculated one above 350 nm. In fact, it displays a slightly higher absorbance and a broadening on the low energy side. Quite remarkably, the broadening toward the low-energy range of the spectrum is less pronounced with respect to the short dyad **D-Ir**, characterized by an absorption extending over 500 nm, see inset of Figure 1. In order to understand this behavior we have to recall that, whereas in $(tpy)_2Ir^{3+}$-type complexes the low-energy absorption band is in general a predominantly LC transition, complexes of the $(tpy)_2Ir^{3+}$-type with benzamide sub-

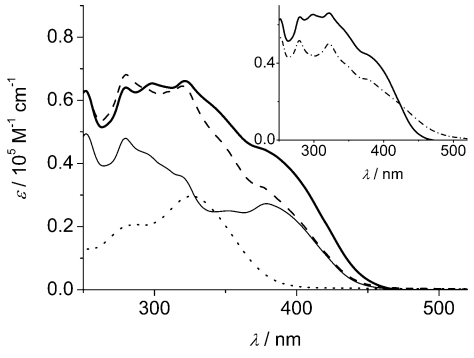

Figure 1. Absorption spectra of the model components and of the arrays. **Ir1** (thin line), **DII** (dotted line), **DII-Ir** (thick line), **Ir1 + DII** (dashed line). Inset: **DII-Ir** (thick line), **D-Ir** (dash-doted line).

stituents were recently demonstrated to exhibit photophysical properties at room temperature typical of a CT state, either of metal-to-ligand charge-transfer nature (MLCT) or of intraligand charge-transfer nature (ILCT).[5,11,12] The presence of an amine electron donor as a substituent can strongly enhance the ILCT nature of the transition, with the terpyridine acting as an electron acceptor and the amine as an electron donor, and further shift the absorbance to the red. From this point of view, interposition of a further amide spacer between the terpyridine acceptor and the aromatic amine donor has the effect of increasing the energy of the band, moving it further to the blue, as noticed in the inset of Figure 1 for **DII-Ir** compared to **D-Ir**.

If we ignore the small perturbation of the spectrum of the Ir unit discussed above, there is no evidence from the spectroscopic data of electronic interactions in the array with respect to the models, in agreement with the electrochemical data. This allows us to use a localized description of the individual subunits in the subsequent discussion of the photoinduced energy and electron-transfer reactions.

Luminescence Spectroscopy

DII emits strongly, with a band maximum at 524 nm, slightly blueshifted with respect to the short analog **D** (λ_{max} = 540 nm); **Ir1** emits moderately with a maximum at 570 nm (Table 2).

Table 2. Luminescence properties in air-equilibrated nitrile solvents. Acetonitrile at 295 K and butyronitrile at 77 K.

	State	295 K			77 K		
		λ_{max} [nm]	τ [ns]	Φ_{em}	λ_{max} [nm]	τ [ns]	E [eV]
Ir1[a,b]	^{3}Ir1	570	490	2.1×10^{-3}	510	80000	2.43
D[b]	^{1}D	540	0.450	0.012	422	2.6	2.93
D-Ir[b]	D-^{3}Ir		–	$\leq6\times10^{-5}$	515[d]	–	2.40
	^{1}D-Ir		$<<$0.01	$\leq6\times10^{-5}$	–	–	
DII[c]	^{1}DII	524	1.0	0.073	414	2.0	2.99
DII-Ir	DII-^{3}Ir[a]	570	–	6×10^{-5}	516		2.40
	^{1}DII-Ir[c]		0.01	5×10^{-4}	400[d]		3.10

[a] Excitation at 430 nm for steady state, for time-resolved determinations excitation at 373 nm. [b] From ref.[7] [c] Excitation at 330 nm for steady state, for time-resolved determinations excitation at 373 nm, 331 nm, or 355 nm. [d] Weak signal.

The luminescence spectra of the array **DII-Ir** at room temperature upon selective excitation of the Ir unit at 430 nm is compared to those of the model **Ir1** absorbing the same number of photons as the unit in the array (Figure 2, right panel). In the left panel of Figure 2 the luminescence detected in the dyad upon excitation at 330 nm, corresponding to excitation of both DII and Ir complex units (absorbing 50% each), is reported and compared to the luminescence from a solution of **DII** absorbing the same number of photons as the unit in the array. The emission of Ir and DII units in the dyad are nearly completely quenched, to ca. 3% and less than 1%, respectively, indicating the occurrence of an efficient quenching process involving both ^{3}Ir and ^{1}DII. It should be noticed that the weak residual luminescence in **DII-Ir** could be due to some very minor, unbound component in the dyad and not to a genuine quenched unit in the array; the definitive answer on the effective quenching of the component in the dyad can only be provided by the time-resolved experiments, discussed below.

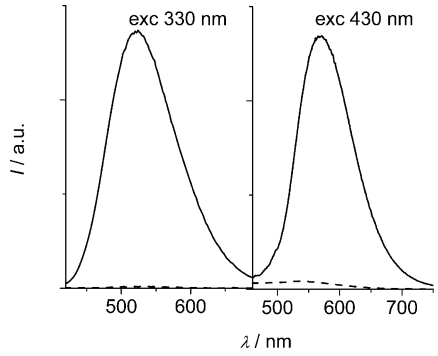

Figure 2. Room-temperature luminescence spectra in acetonitrile. Left panel: excitation at 330 nm, 50% excitation of DII and Ir components, **DII** (solid line) A = 0.056, **DII-Ir** (dashed line) A = 0.12. Right panel: selective excitation at 430 nm of Ir component, **Ir1** (solid line), A = 0.13, **DII-Ir** (dashed line) A = 0.13. The absorbance of the solutions is arranged to provide the absorption of the same number of photons in the model and in the corresponding unit in the array.

Luminescence spectra of the models **Ir1** and **DII** at 77 K in a glassy butyronitrile matrix display emission maxima at 414 and at 510 nm, respectively, with a remarkable hypsochromic shift from fluid (295 K) to rigid (77 K) solvent (see Table 2). This can be explained by a strong CT character for the ^{1}DII emitting excited state which is less stabilized in a rigid medium; in the case of **Ir1**, a change in the spectral profile is also detected (compare Figures 2 and 3), indicative of a switching of the excited-state nature from a room-temperature CT to a predominantly ligand-centered state in the glass, as previously discussed.[11]

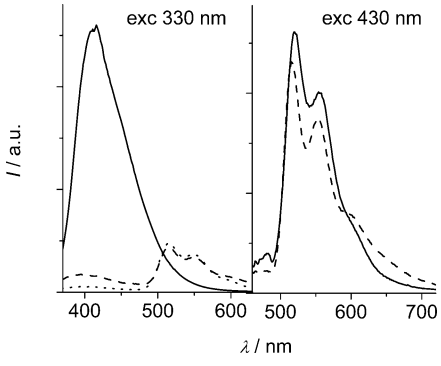

Figure 3. Luminescence spectra in butyronitrile at 77 K. Left panel: excitation at 330 nm, 50% excitation of DII and Ir components, **DII** (solid line) A = 0.1, **Ir1** (dotted line) A = 0.1, **DII-Ir** (dashed line) A = 0.2. Right panel: selective excitation at 430 nm of Ir component, **Ir1** (solid line) A = 0.08, **DII-Ir** (dashed line) A = 0.08. The absorbance of the solutions is arranged to provide the absorption of the same number of photons in the model and in the corresponding unit in the array.

Luminescence experiments on the models and **DII-Ir** in butyronitrile glass at 77 K show that nearly no quenching of the Ir unit occurs at 77 K, whereas the DII unit is still strongly quenched also at 77 K, as evidenced in Figure 3 which compares the luminescence from **DII** and **Ir1** solutions to that from **DII-Ir** after selective excitation of the Ir complex unit at 430 nm in the right panel, or of the DII and Ir components (absorbing 50% each) at 330 nm in the left panel. With respect to the results previously reported for the short corresponding dyad **D-Ir** both at room temperature and at 77 K, in **DII-Ir** the luminescence quenching is less effective. This is in agreement with a slower electron transfer over the longer bridge connecting the donor to the Ir complex.

The luminescence lifetimes of the model **Ir1** in air-equilibrated acetonitrile solution determined by a single photon nanosecond apparatus, is 490 ns.[7] Any attempt to determine the lifetime of the Ir unit in the dyad was unsuccessful at room temperature, neither a single-photon counting technique with 0.3 ns resolution, nor a streak-camera detection with 10 ps resolution allowed any emission to be registered. Given the very low radiative rate constant of the Ir complex, $k_r \approx 5 \times 10^3$ s^{-1} ($k_r = \phi/\tau$), a technique like the single-shot streak camera is not convenient for detecting such low emissions, therefore we cannot exclude for the ^{3}Ir component in **DII-Ir** a lifetime shorter than 0.3 ns. Only the time-resolved absorption data discussed below will clear this point. The strong emission of **DII** was time-resolved by a picosecond streak camera after excitation at 355 nm and displays a lifetime of 1.0 ns. This luminescence is quenched in **DII-Ir** and displays a time profile very similar to the instrumental response (Figure 4) from which a lifetime of ca. 10 ps can be calculated by deconvolution with the instrumental profile. This value is in reasonable agreement with steady-state data, which indicates a reduction in the emission yield of the order of 1% in passing from the **DII** model to the dyad **DII-Ir**. In the case of the short dyad **D-Ir**, no luminescence could be detected from the D component, confirming a more efficient quenching due to electron transfer responsible for charge separation and allowing us to set an upper limit to the lifetime of $\tau << 10$ ps.

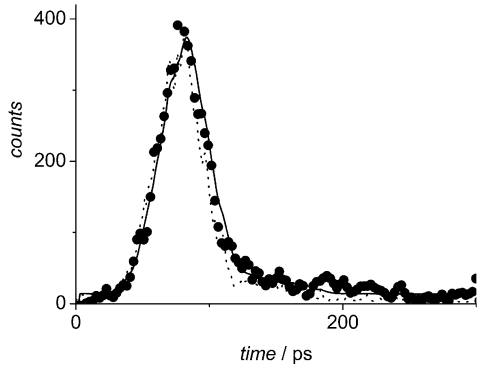

Figure 4. Luminescence registered at 520 nm from **DII-Ir** acetonitrile solution after excitation with a laser pulse (35 ps, 355 nm, 1 mJ) (full circles) with the instrumental pulse profile (dotted line) and the fitting (solid line).

Time-resolved experiments at 77 K in butyronitrile glass allowed the following parameters to be measured. The lifetime of the models **D** and **DII** are 2.6 and 2 ns, respectively, showing a slight temperature dependence. On the contrary, the lifetime of **Ir1** at 77 K is 80 μs, much longer than at room-temperature (Table 2). This has to be assigned to a switch in the nature of the excited state when the medium becomes rigid from ^{3}CT, very likely of intra-ligand charge-transfer nature, to a ^{3}LC, as already discussed above. In the dyad **DII-Ir**, the lifetime of Ir measured with a time-correlated single photon apparatus is 56 μs compared to the 80 μs of the model, confirming a very modest quenching in agreement with steady-state experiments. The DII unit decay in the dyad **DII-Ir** at 77 K was still extremely fast and of the same order as the exciting profile; an accurate determination of the lifetime was precluded by the strong light scattering in the glass. From the short counterpart **D-Ir** no luminescence could be detected similarly to what occurs at room temperature.

Transient Absorption Spectroscopy

Valuable information on the products of electron transfer can be gained by transient absorption techniques. The chemically generated cation DII$^+$ (see Exp. Sect. for details) has a peak at 760 nm ($\varepsilon \approx 27400$) and a minor broad band at 590 nm, in agreement with previous reports.[13] It should be noted that at the excitation wavelength, 355 nm, both units of the **DII-Ir** dyad absorb light with the following probability (see Figure 1): 60% for Ir, 40% for D.

The end of pulse transient absorption spectra detected with picosecond resolution of optically matched solutions of the models and **DII-Ir** are reported in Figure 5. **Ir1** displays a strong absorption band with a broad maximum around 780 nm assigned to ^{3}Ir1, stable on the 3 ns window of the experiment. **DII** displays a sharp band at 750 nm with a lifetime of ca. 900 ps, in reasonable agreement with the luminescence lifetime of 1.0 ns, indicating that the detected species is the singlet excited state ^{1}DII.[14] The time-resolved spectrum of **DII-Ir** has a maximum at 765 nm which, for similarity with the spectrum of D$^+$-Ir$^-$ (λ_{max} = 765 nm) and with the chemically generated spectrum of DII$^+$, is assigned to the CS state DII$^+$-Ir$^-$. No trace of the spectral features of DII, which has in fact been shown by luminescence experiments to decay with a lifetime of 10 ps, i.e. during the laser pulse, is detected. Similarly, no absorbance ascribable to ^{3}Ir, which would be easily identifiable because of its broad and intense spectrum, appears at the end of the pulse. This set up the unsolved problem of the lifetime of DII-^{3}Ir species, which could not be unambiguously determined by luminescence techniques (see above). By transient absorbance experiments we can set an upper limit of 20 ps for the lifetime of DII-^{3}Ir, a longer lifetime of this species would in fact cause the appearance in the spectrum registered at the end of the pulse of the typical features of the ^{3}Ir absorbance (see Figure 5) which are, on the contrary, absent. The time evolution of the spectrum, re-

ported in Figure 6 with the extracted time profile, allows us to derive a lifetime of the CS state of 210 ps. The absorbance decays to the baseline without leaving any residual absorbance in the longer timescale, as confirmed by nanosecond flash-photolysis experiments on **DII-Ir**. No residual absorbance in the nanosecond time scale can be detected for **DII** either, on the contrary nanosecond flash-photolysis experiments allow us to detect in **Ir1** solutions the full evolution of the ^{3}Ir1 species in air-equilibrated samples which has a lifetime of 440 ns, in good agreement with the luminescence lifetime.

The singlet excited state ^{1}D derived from the component **D** displayed an identical absorption spectrum but a shorter lifetime of 490 ps and, as far as the CS state is concerned, DII$^+$-Ir$^-$ has a nearly identical spectrum but a much longer lifetime than D$^+$-Ir$^-$ (70 ps).

The transient absorbance data for the models, **D-Ir** and **DII-Ir** are collected in Table 3.

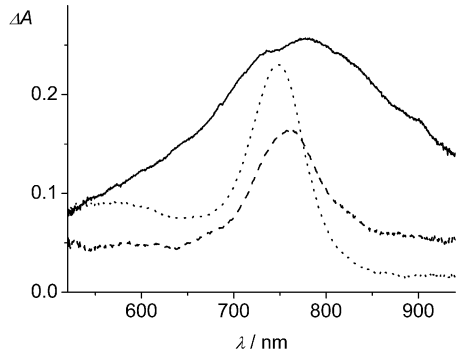

Figure 5. End of pulse absorption spectra of **Ir1** (solid line), **DII** (dotted line), and **DII-Ir** (dashed line) in acetonitrile solutions upon excitation at 355 nm (2.8 mJ/pulse, 35 ps pulse). All solutions had A = 0.51 at the exciting wavelength.

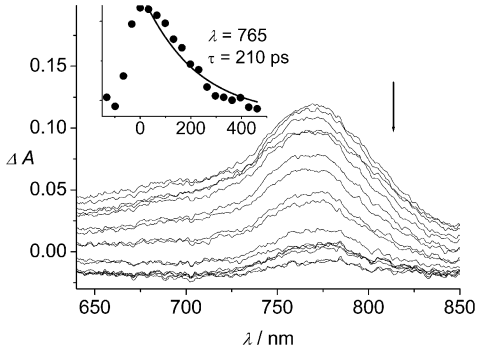

Figure 6. Time evolution of the transient spectrum of **DII-Ir** in acetonitrile (2.5 mJ, A = 0.5); spectra taken with delays of 165 ps. In the inset, the time evolution of the absorbance at 765 nm and exponential fitting are shown.

Table 3. Transient absorption data at room temperature (excitation at 355 nm) in air-equilibrated acetonitrile solutions of **DII-Ir**, **D-Ir**, and models.

	State	λ_{max} [nm]	τ [ns]
Ir1[a]	^{3}Ir1	780	440
D[a]	^{1}D	750	0.49
D-Ir[a]	D-^{3}Ir	–	<0.02
	^{1}D-Ir	–	<0.02
	D$^+$-Ir$^-$	765	0.070
DII	^{1}DII^c	750	0.90
DII-Ir	DII-^{3}Ir	–	<0.02
	^{1}DII-Ir		<0.02
	DII$^+$-Ir$^-$	765	0.210

[a] From ref.[7]

Photoinduced Processes

Scheme 4 shows the energy level diagrams of the present **DII-Ir** dyad and of the corresponding short dyad **D-Ir** [7] and can help to discuss and compare the processes in the two cases.

These diagrams can be drawn from the luminescence data collected in Table 2 and from the electrochemical data reported in Table 1. The excited-state energies are derived from the maxima of the emission at 77 K (Table 2), whereas the charge-separated state energy levels are calculated by simply adding the energy necessary to oxidize the potential donor and the energy necessary to reduce the potential acceptor in acetonitrile (Table 1) without further corrections.

Both dyads are made of an easy to oxidize D or DII component ($E_{1/2}$ = +0.75 V and $E_{1/2}$ = +0.76 V in the pertinent dyads, respectively) and of the iridium complex which can be reduced at low potentials ($E_{1/2}$ = –0.75 V in the short and $E_{1/2}$ = –0.78 V in the long dyad) yielding charge-separated states D$^+$-Ir$^-$ or DII$^+$-Ir$^-$ with an energy of 1.51 and 1.54 eV, respectively (Table 1). These are characterized by an extra electron localized on the metal complex, most probably on the ligand, and a hole on the triphenylamine donor. Charge separation is feasible both from the excited donor, ^{1}DII-Ir (^{1}D-Ir) and from the excited acceptor DII-^{3}Ir (D-^{3}Ir) but the excited state quenching mechanism in the two cases will be different. When Ir is excited, a reductive quenching of its excited state will occur, i.e. the electron will move from the HOMO localized on the donor to the HOMO localized on the Ir complex, with ΔG^0 = –0.9 and –0.86 eV for **D-Ir** and **DII-Ir**, respectively. When the donor is excited, an electron will move from the LUMO localized on DII to the LUMO on the Ir complex acceptor, with ΔG^0 = –1.43 eV for **D-Ir** and ΔG^0 = –1.56 eV for **DII-Ir**. Both types of electron transfer take place at room temperature, as testified by the quenching of the luminescent states localized on both units as shown in Figures 2 and 4.

We cannot exclude the possibility of an energy transfer from ^{1}DII-Ir to DII-^{3}Ir, which is spin-forbidden but could be made possible by the strong spin-orbit coupling induced by the heavy Ir ion. The overall result would be undistinguishable from a direct electron transfer from the excited state localized on the donor; however, the 77 K experiment seems to indicate that such an energy transfer (expected to be little affected by temperature) does not take place. In the latter case in fact we would expect a sensitization of the Ir luminescence upon excitation of the DII unit at 330 nm,

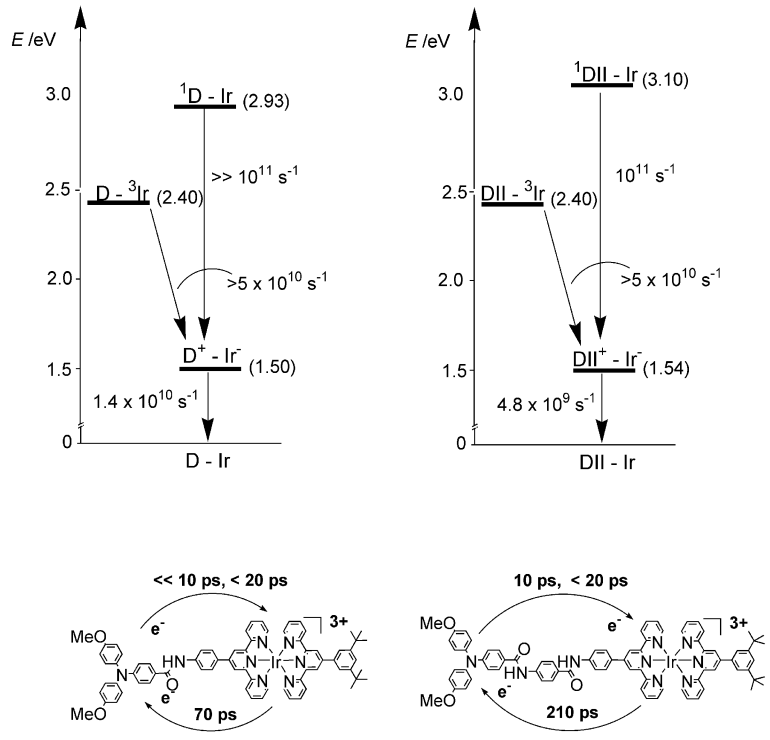

Scheme 4. Energy-level diagrams and schematic representation of the processes for **D-Ir** and **DII-Ir**.

which does not occur (see Figure 3). Therefore, the following discussion will not take the spin-forbidden energy transfer process into account.

Whereas we could measure the reaction rate of ^{1}DII-Ir → DII$^+$-Ir$^-$, $k_{cs} = 10^{11}$ s^{-1}, corresponding to the lifetime of 10 ps, for the DII-^{3}Ir → DII$^+$-Ir$^-$ reaction we could only set a lower limit, $k_{cs} > 5 \times 10^{10}$ s^{-1}, based on the results of the transient absorbance (see above). In the short dyad **D-Ir**, similar results were obtained for the D-^{3}Ir → D$^+$-Ir$^-$ reaction, for which an identical lower limit of the rate constant $k_{cs} > 5 \times 10^{10}$ s^{-1}, corresponding to the time resolution of the transient absorbance experiment, was set. For the ^{1}D-Ir → D$^+$-Ir$^-$ step, the improved time resolution of the apparatus with respect to previously reported data ($k_{cs} > 5 \times 10^{10}$ s^{-1})[15] allowed us to set a limit of $k_{cs} > 10^{11}$ s^{-1}. The driving force of the charge-separation reactions are not very different in going from the short to the long dyad, but the distance between the donor and acceptor changes remarkably, from 1.65 to 2.3 nm. Therefore, a slower charge separation step ^{1}DII-Ir → DII$^+$-Ir$^-$ compared to ^{1}D-Ir → D$^+$-Ir$^-$ can be measured. On the contrary, for the charge separation starting from the excited state of the Ir metal complex, either DII-^{3}Ir → DII$^+$-Ir$^-$ or D-^{3}Ir → D$^+$-Ir$^-$, it is difficult to make comparisons since the same lower limit for the rate constant has been determined. Overall, a slight decrease in the rate of charge separation can be registered in **DII-Ir** compared to **D-Ir**; however, the yield of charge separation – $\phi_{cs} = k_{cs}/\Sigma k = k_{cs}/(k_{cs} + 1/\tau_0)$, where τ_0 is the lifetime of the excited state in the models – is still of the order of 99% when starting from ^{1}DII-Ir (τ_0 = 1 ns) and nearly 100% when starting from DII-^{3}Ir (τ_0 = 490 ns in air). Thus, the insertion of a further benzamide group between the donor and acceptor is not too detrimental to the charge-separation process at room temperature. This is different at 77 K, where the absence of quenching of the Ir component and the persistence of the quenching of the D unit in the dyad at 77 K indicate that electron transfer from DII-^{3}Ir is inefficient and only electron transfer from ^{1}DII-Ir continues to be operative with a still remarkable rate of the order of 20 ps (Figure 3 and Table 2). This can be understood if one considers that the rigidity of the medium, preventing solvent molecule reorganization around the CS state, destabilizes the CS level by a value which can be quite high[16] and decreases the driving force for electron-transfer reactions originating from the DII-^{3}Ir and the ^{1}DII-Ir states. Under these conditions, the lowest-lying DII-^{3}Ir (ca. 2.4 eV) is unable to transfer an electron, whereas the higher ^{1}DII-Ir (ca. 3 eV) has sufficient driving force to transfer the electron also in rigid media at 77 K.

Once the charge-separated state DII$^+$-Ir$^-$ is formed, it decays to the ground state with a lifetime of 210 ps, three-times shorter than D$^+$-Ir$^-$ which has a lifetime of 70 ps. The driving force of the charge-recombination reaction is high, leading us to assume a Marcus-inverted behavior, i.e. the rate slows as the driving force increases.[17] The driving force is slightly higher for **DII-Ir** compared to **D-Ir** (ΔG^0 = –1.54 eV for the long dyad against ΔG^0 = –1.50 eV), but most importantly the insertion of a further benzamide group is effective in electronically decoupling the donor and acceptor units in the long dyad and decreases the charge-recombination rate. The increase from 70 to 210 ps lifetime in passing from **D-Ir** to the long **DII-Ir** dyad, suggests that

a newly synthesized long triad DII-Ir-A could be more efficient in producing charge separation over the terminal components. In the **D-Ir-A** triad, as discussed above, the poor efficiency of charge separation was due to the fast step ($k = 1.4 \times 10^{10}\ s^{-1}$) preferably leading D^+-Ir^--A to the ground state rather than to the fully CS state D^+-Ir-A^- by a further electron transfer step ($k = 2.4 \times 10^9\ s^{-1}$). The decrease of the charge recombination step in DII^+-Ir^--A ($k = 4.8 \times 10^9\ s^{-1}$), assuming that the rest of the triad is unchanged with respect to the previously studied **D-Ir-A** triad, would allow us to reach an efficiency of charge separation of the order of 30%. This would be a noticeable improvement with respect to the yield of ca. 10% achieved in the short triad **D-Ir-A** and, if we consider that due to the increased donor–acceptor distance an even longer lifetime of the final CS would be expected in a long triad DII-Ir-A, the demanding synthesis of this structure could be undertaken with some degree of confidence in satisfactory performances.

Conclusions

We have synthesized a new dyad **DII-Ir** made of a triphenylamine donor and of a bis(terpyridine)Ir^{III} acceptor separated by a bridge composed of two benzamide groups, and we have studied the photoinduced processes. The properties of the dyad have been compared to those of a corresponding dyad **D-Ir** characterized by a bridge connecting the donor and the acceptor consisting of a single benzamide unit. We showed that, whereas the charge-separation steps are still very efficient in the long dyad (≥99%), *charge recombination is slowed by a factor of three with respect to the short dyad*. This is promising and encourages the use of this dyad in the assembly of the more elaborate array DII-Ir-A. This would simply have a further benzamide unit in the spacer connecting DII to Ir, with respect to the already studied **D-Ir-A** triad of Scheme 1 for which an unsatisfactory yield of ca. 10% of charge separation was reported. In the long triad DII-Ir-A, a lifetime of the CS state DII^+-Ir^--A of the order of 210 ps would be expected, similar to the dyad studied here. This would decrease the competition of the recombination to the ground state with respect to the further electron-transfer step leading to full charge separation over the extreme components with an efficiency of the order of 30% with respect to the ca. 10% of the previously studied **D-Ir-A** triad. It should also be stressed that, due to the increased D–A distance, an even longer lifetime of the final CS state, with respect to the 120 μs of the short **D-Ir-A** triad, is expected.

Experimental Section

General: ^1H NMR spectra were acquired either with a Bruker WP 200 SY, a Bruker AC300, or a Bruker AM 400 spectrometer, using the deuterated solvent as the lock and residual solvent as the internal reference (CD_3CN: δ = 1.96 ppm; [D_6]DMSO: δ = 2.52 ppm). Electron spray ionization mass spectra (ESI-MS) were recorded with a Bruker MicroTOF instrument. Cyclic voltammetry experiments were performed using an EG&G 273A potentiostat, a Pt working electrode, a Pt counter-electrode, a KCl-saturated calomel electrode (SCE) as a reference, and 0.1 M nBu_4NPF_6 in CH_3CN as the supporting electrolyte. The typical sweep rate was 100 mV/s.

Starting Compounds: [4′-(3,5-Di-*tert*-butylphenyl)-2,2′:6′,2′′-terpyridine]$IrCl_3$,[5a] tpy-ph-NH_2,[9] 4-[bis(4-methoxyphenyl)amino]benzoic acid, **DII** and **Ir1**[7] were prepared according to the published procedures.

1: terpy-ph-NH_2 (500 mg, 1.54 mmol) was dissolved in dimethylacetamide (8 mL), after which some pyridine (2 mL) was added. Upon addition of *p*-nitrobenzoyl chloride (410 mg, 2.2 mmol, excess), the color of the solution immediately turned from pale yellow to deep yellow. After stirring at room temperature for 28 h, the reaction mixture was added dropwise to cold Et_2O and was placed in the freezer for 30 min to induce precipitation. The dark yellow precipitate of **1** was filtered off and dried under vacuum. Yield: 95% (700 mg). $C_{28}H_{19}N_5O_3$ (473.48): calcd. C 71.03, H 4.04, N 14.79; found C 71.45, H 4.03, N 14.47. ^1H NMR ([D_6]DMSO, 200 MHz): δ = 10.87 (s, 1 H, NH), 8.86–8.83 (m, 6 H, 6-H, 3-H, 3′-H, 5′-H), 8.44–8.08 (m, 10 H, o1-H, m1-H, o2-H, m2-H, 4-H), 7.72–7.65 (m, 2 H, 5-H) ppm. ^{13}C NMR ([D_6]DMSO, 75 MHz): δ = 164.1, 153.5, 152.6, 149.6, 149.3, 147.6, 147.5, 140.5, 140.3, 132.0, 129.4, 127.7, 125.6, 123.6, 122.4, 120.9, 118.9 ppm. ES-MS: *m*/*z* (calcd.) = 474.16 (474.15) $[M + H]^+$.

2: Compound **1** (230 mg; 0.49 mmol) was suspended in refluxing MeOH/THF (1:1, v/v; 100 mL). Pd/C 5% (108 mg) was added as a solid, and a mixture of hydrazine monohydrate (0.5 mL) in MeOH (5 mL) was added dropwise over a period of 10 min. After the addition, the colorless solution was refluxed for 40 min, cooled to room temperature, filtered through Celite, and concentrated. After one night in the refridgerator, the precipitate was filtered off and washed with water, MeOH, and Et_2O. Compound **2** was obtained as a colorless solid. Yield: 97% (210 mg). $C_{28}H_{21}N_5O$ (443.50): calcd. C 75.83, H 4.77, N 15.79; found C 74.14, H 4.63, N 15.20. ^1H NMR ([D_6]DMSO, 200 MHz): δ = 10.02 (s, 1 H, NH), 8.79 (dd, ^4J = 4.7, ^5J = 0.8 Hz, 2 H, 6-H), 8.75 (s, 2 H, 3′-H, 5′-H), 8.70 (d, ^3J = 7.9 Hz, 2 H, 3-H), 8.06 (m, 2 H, 4-H), 8.00 (m, 2 H, o1-H, m1-H), 7.79 (d, ^3J = 8.6 Hz, 2 H, o2-H), 7.55 (ddd, ^3J = 7.5, ^4J = 4.7, ^5J = 1.0 Hz, 2 H, 5-H), 6.64 (d, ^3J = 8.6 Hz, 2 H, m2-H) ppm. ^{13}C NMR ([D_6]DMSO, 75 MHz): δ = 161.5, 152.0, 151.5, 148.8, 145.7, 145.4, 137.7, 133.8, 127.8, 125.9, 123.5, 120.9, 117.3, 117.2, 116.9, 113.7, 108.9 ppm. ES-MS: *m*/*z* (calcd.) = 444.18 (443.17) $[M + H]^+$.

3: DMAP (470 mg, 3.64 mmol, 3.3 equiv.) and EDC (420 mg, 2.20 mmol, 1.9 equiv.) were added to a solution of 4-[bis(4-methoxyphenyl)amino]benzoic acid (634 mg, 1.81 mmol, 1.5 equiv.) in freshly distilled CH_2Cl_2 (6 mL). After a few minutes of stirring, the solution was deep yellow. **2** (500 mg, 1.13 mmol) and DMF (1 mL) were added, and the reaction mixture was stirred under argon at 40 °C for 10 h. CH_2Cl_2 was removed under reduced pressure. Water and saturated $NaHCO_3$ solution (25 mL each) were added resulting in a pale yellow precipitate which was filtered off and washed with $NaHCO_3$ solution, water and then with a mixture of CH_2Cl_2/Et_2O (1:1, v/v) to afford **3** as a pale yellow solid in 71% yield (626 mg, 0.81 mmol). $C_{49}H_{38}N_6O_4$ (774.86): calcd. C 75.95, H 4.94, N 10.85; found C 74.97, H 4.76, N 10.46. ^1H NMR ([D_6]DMSO, 300 MHz): δ = 10.37 (s, 1 H, NH), 10.23 (s, 1 H, NH), 8.78 (d, ^3J = 4.1 Hz, 2 H, 6-H), 8.70 (s, 2 H, 3′-H, 5′-H), 8.68 (d, ^3J = 7.9 Hz, 2 H, 3-H), 8.08–8.94 (m, 10 H, 4-H, o3-H, m3-H, o4-H, m4-H), 7.82 (d, ^3J = 8.9 Hz, 2 H, o5-H), 7.54 (ddd, ^3J = 7.5, ^3J = 4.9, ^4J = 1.1 Hz, 2 H, 5-H), 7.14 (d, ^3J = 9.0 Hz, 4 H, a-H), 6.98 (d, ^3J = 9.0 Hz, 4 H, b-

H), 6.74 (d, ^3J = 8.9 Hz, 2 H, m5-H), 3.77 (s, 6 H, CH_3) ppm. ES-MS: *m*/*z* (calcd.) = 775.31 (775.30) $[M + H]^+$.

DII-Ir: A suspension of [4′-(3,5-di-*tert*-butylphenyl)-2,2′:6′,2′′-terpyridine]$IrCl_3$ (48 mg, 0.067 mmol) and **3** (51 mg, 0.066 mmol) in ethylene glycol (15 mL) was homogenized under ultrasound during 25 min, then heated at 160 °C during 20 min under argon. The crude product was precipitated with a saturated solution of KPF_6, filtered off, and purified on silica ($CH_3CN/H_2O/KNO_3$, 100:0:0 to 100:7:0.7). After anion exchange, **DII-Ir** was obtained as a yellow solid. Yield: 70% (85 mg). ^{1}H NMR (CD_3CN, 400 MHz): δ = 9.15 (s, 1 H, 1-NH), 9.10 (s, 2 H, 3′-D, 5′-D), 9.04 (s, 2 H, 3′-H, 5′-H), 8.82 (s, 1 H, 2-NH), 8.78 (dd, ^3J = 8.2, ^4J = 0.7 Hz, 2 H, 3-H), 8.73 (dd, ^3J = 8.2, ^4J = 0.7 Hz, 2 H, 3-D), 8.29–8.22 (m, 6 H, 4-H, 4-D, o3-H), 8.19 (d, ^3J = 8.9 Hz, 2 H, m3-H), 8.02 (d, ^3J = 8.8 Hz, 2 H, o4-H), 7.99 (d, ^4J = 1.7 Hz, 2 H, o-H), 7.90 (d, ^3J = 8.8 Hz, 2 H, m4-H), 7.87 (t, ^4J = 1.7 Hz, 1 H, p-H), 7.77–7.69 (m, 6 H, o5-H, 6-H, 6-D), 7.52–7.47 (m, 4 H, 5-H, 5-D), 7.17 (d, ^3J = 8.9 Hz, 4 H, a-H), 6.96 (d, ^3J = 8.9 Hz, 4 H, b-H), 6.7 (d, ^3J = 8.9 Hz, 2 H, m5-H), 3.80 (s, 6 H, CH_3), 1.52 (s, 18 H, *t*Bu) ppm. HR ES-MS: *m*/*z* (calcd.) = 1678.4467 (1678.4387) $[M - PF_6]^+$.

The **DII$^+$** species was generated by the addition of one drop of Br_2 to a solution of **DII** (2.5×10^{-4} M, 2 mm optical path) in acetonitrile, the calculated molar absorption coefficient assuming complete conversion of the starting **DII** was ε = 27400 $M^{-1}cm^{-1}$ at 760 nm.

For the photophysical experiments, the solvents were spectrophotometric-grade acetonitrile at 295 K and butyronitrile at 77 K. If not otherwise specified, solutions were at ambient temperature and air-equilibrated. Standard 10 mm fluorescence cells were used at 295 K whereas experiments at 77 K made use of capillary tubes in a home-made quartz Dewar filled with liquid nitrogen. Because of geometrical irradiation conditions at 77 K the absolute quantum yield could not be determined, but the relative emission yields could be derived with some confidence. When necessary, solutions were bubbled for 10 min with a stream of argon in home-modified 10 mm fluorescence cells. A Perkin–Elmer Lambda 9 UV/Vis spectrophotometer and a Spex Fluorolog II spectrofluorimeter were used to acquire absorption and emission spectra. Emission quantum yields were determined after correction for the photomultiplier response, with reference to air-equilibrated (3,5-di-*tert*-butylphenyl-2,2′;6′,2′′-terpyridine)$_2$Ir^{III}$(PF_6)_3$ with ϕ_{em} = 0.022 in air-saturated acetonitrile.[5a] Luminescence lifetimes (τ) were obtained with IBH single-photon counting equipment upon excitation at 373 and 331 nm from a pulsed diode source or with an apparatus based on an Nd:YAG laser (35 ps pulse duration, 355 nm, 0.5 mJ) and a Streak Camera with an overall resolution of 10 ps.[18] Transient absorbance in the picosecond range made use of a pump and probe system based on an Nd-YAG laser (Continuum PY62/10, 35 ps pulse). The third harmonic (355 nm) at a frequency of 10 Hz and an energy of ca. 3 mJ/pulse was used to excite the samples whose absorbance at the excitation wavelength was ca. 0.6. The residual 1064 nm light (ca. 40 mJ) was focused on a stirred 10 cm cell containing a mixture of D_2O/D_3PO_4 to produce a white light continuum which was used as analyzing light. A computer-controlled optical delay stage (Ealing) on the path of the excitation beam provided a delay between excitation and analysis. The analyzing light was split into two parts probing irradiated and un-irradiated portions, respectively, of the sample and crossed the sample cell in a nearly collinear geometry with respect to the excitation beam. The transmitted probes were fed through optical fibers into a spectrograph (Spectrapro 275, Acton) and were detected in two separate regions of a CCD detector (Princeton Instruments). The control units for the delay line, for the spectrograph and for the CCD detector were driven by customized software (Eurins) which also allowed us to acquire spectra at increasing time delays between the pump and the probe. Typically, 200–500 laser shots were collected and averaged to obtain a single spectrum at a specific time delay. Kinetic analyses were made by selecting the absorbance values of successive time-resolved spectra at the selected wavelength and by applying standard iterative procedures. More details can be found elsewhere.[19]

Nanosecond laser flash photolysis experiments were performed by a system based on an Nd-YAG laser (JK Lasers, 355 nm, 1.5–8.5 mJ, 18 ns pulse) previously described using a right-angle analysis on the excited sample.[20] Experimental uncertainties are estimated to be within 10% for lifetime determination involving simple exponential, 20% for lifetime determinations involving multiple exponentials or more complex kinetics, 15% for quantum yields, 20% for molar absorption coefficients and 3 nm for emission and absorption peaks. Molecular dimensions were estimated after MM2 energy minimization from CS Chem3D Ultra software.

Supporting Information (see footnote on the first page of this article): Atom numbering scheme for compounds **1**, **2**, **3**, and **DII-Ir**.

Acknowledgments

We thank Consiglio Nazionale delle Ricerche of Italy (PM-P04-010, MACOL), Centre National de la Recherche Scientifique (France), Ministero dell'Istruzione, dell'Universita' e della Ricerca of Italy, and COST D31 for financial support.

[1] a) D. Gust, T. A. Moore, A. L. Moore, A. N. Macpherson, A. Lopez, J. M. DeGraziano, I. Gouni, E. Bittersman, G. R. Seely, F. Gao, R. A. Nieman, X. C. Ma, L. J. Demanche, S.-C. Hung, D. K. Luttrull, S.-J. Lee, P. K. Kerrigan, *J. Am. Chem. Soc.* **1993**, *115*, 11141–11152; b) K. A. Joliffe, T. D. Bell, K. P. Ghiggino, S. J. Langford, M. N. Paddon-Row, *Angew. Chem.* **1998**, *110*, 960–963; *Angew. Chem. Int. Ed. Engl.* **1998**, *37*, 916–919; c) H. Imahori, D. M. Guldi, K. Tamaki, Y. Yoshida, C. Luo, Y. Sakata, S. Fukuzumi, *J. Am. Chem. Soc.* **2001**, *123*, 6617–6628; d) H. Imahori, Y. Sekiguchi, Y. Kashiwagi, T. Sato, Y. Araki, O. Ito, H. Yamada, S. Fukuzumi, *Chem. Eur. J.* **2004**, *10*, 3184–3196.

[2] a) T. J. Meyer, *Acc. Chem. Res.* **1989**, *22*, 163–170; b) J. H. Alstrum-Acevedo, M. K. Brennaman, T. J. Mayer, *Inorg. Chem.* **2005**, *44*, 6802–6827; c) L. De Cola, V. Balzani, F. Barigelletti, L. Flamigni, P. Belser, A. von Zelewsky, M. Frank, F. Vogtle, *Inorg. Chem.* **1993**, *32*, 5228–5238; d) I. M. Dixon, J.-P. Collin, J.-P. Sauvage, L. Flamigni, *Inorg. Chem.* **2001**, *40*, 5507–5517; e) C. Chiorboli, S. Fracasso, F. Scandola, S. Campagna, S. Serroni, R. Konduri, F. M. MacDonnell, *Chem. Commun.* **2003**, *14*, 1658–1659; f) S. Chakraborty, T. J. Wadas, H. Hester, R. Schmehl, R. Eisenberg, *Inorg. Chem.* **2005**, *44*, 6865–6878; g) M. Borgström, N. Shaikh, O. Johansson, M. F. Anderlund, S. Styring, B. Åkermark, A. Magnuson, L. Hammarström, *J. Am. Chem. Soc.* **2005**, *127*, 17504–17515.

[3] a) L. Flamigni, I. M. Dixon, J.-P. Collin, J.-P. Sauvage, *Chem. Commun.* **2000**, 2479–2480; b) I. M. Dixon, J.-P. Collin, J.-P. Sauvage, F. Barigelletti, L. Flamigni, *Angew. Chem. Int. Ed.* **2000**, *39*, 1292–1295.

[4] a) L. Flamigni, G. Marconi, I. M. Dixon, J.-P. Collin, J.-P. Sauvage, *J. Phys. Chem. B* **2002**, *106*, 6663–6671; b) E. Baranoff, K. Griffiths, J.-P. Collin, J.-P. Sauvage, B. Ventura, L. Flamigni, *New J. Chem.* **2004**, *28*, 1091–1095.

[5] a) J.-P. Collin, I. M. Dixon, J.-P. Sauvage, J. A. G. Williams, F. Barigelletti, L. Flamigni, *J. Am. Chem. Soc.* **1999**, *121*, 5009–5016; b) I. M. Dixon, J.-P. Collin, J.-P. Sauvage, L. Flamigni, S. Encinas, F. Barigelletti, *Chem. Soc. Rev.* **2000**, *29*, 385–391.

[6] E. Baranoff, J.-P. Collin, L. Flamigni, J.-P. Sauvage, *Chem. Soc. Rev.* **2004**, *33*, 147–155.
[7] L. Flamigni, E. Baranoff, J.-P. Collin, J.-P. Sauvage, *Chem. Eur. J.* **2006**, *12*, 6592–6606.
[8] E. Baranoff, I. M. Dixon, J.-P. Collin, J.-P. Sauvage, B. Ventura, L. Flamigni, *Inorg. Chem.* **2004**, *43*, 3057–3066.
[9] P. Lainé, F. Bedioui, P. Ochsenbein, V. Marvaud, M. Bonin, E. Amouyal, *J. Am. Chem. Soc.* **2002**, *124*, 1364–1277.
[10] J. C. Sheehan, P. A. Cruickshank, G. L. Broshart, *J. Org. Chem.* **1961**, *26*, 2525–2528.
[11] L. Flamigni, B. Ventura, F. Barigelletti, E. Baranoff, J.-P. Collin, J.-P. Sauvage, *Eur. J. Inorg. Chem.* **2005**, 1312–1318.
[12] W. Leslie, A. S. Bastanov, J. A. K. Howard, J. A. G. Williams, *Dalton Trans.* **2004**, 623–631.
[13] R. I. Walter, *J. Am. Chem. Soc.* **1966**, *88*, 1923–1930.
[14] Some instability was displayed by the **DII** solution under the harsh laser energy conditions of the pump and probe experiment.
[15] Since previously reported experiments the time resolution of the luminescence experiments was improved from 20 ps to 10 ps, due to a better deconvolution procedure of the signal with the instrumental response.
[16] a) Values as high as 0.8 eV have been reported, see, for example: G. L. Gaines III, M. P. O'Neil, W. A. Swec, M. P. Niemczyk, M. R. Wasielewski, *J. Am. Chem. Soc.* **1991**, *113*, 719–721; b) L. Hammarström, F. Barigelletti, L. Flamigni, N. Armaroli, A. Sour, J.-P. Collin, J.-P. Sauvage, *J. Am. Chem. Soc.* **1996**, *118*, 11972–11973 and references cited therein.
[17] a) R. A. Marcus, N. Sutin, *Biochim. Biophys. Acta* **1985**, *811*, 265; b) R. A. Marcus, *Angew. Chem. Int. Ed. Engl.* **1993**, *32*, 1111.
[18] L. Flamigni, *J. Phys. Chem.* **1993**, *97*, 9566–9572.
[19] a) B. Ventura, A. Degli Esposti, B. Koszarna, D. T. Gryko, L. Flamigni, *New J. Chem.* **2005**, *29*, 1559–1566; b) L. Flamigni, N. Armaroli, F. Barigelletti, V. Balzani, J.-P. Collin, J.-O. Dalbavie, V. Heitz, J.-P. Sauvage, *J. Phys. Chem. B* **1997**, *101*, 5936–5943.
[20] a) L. Flamigni, *J. Phys. Chem.* **1992**, *96*, 3331–3337; b) L. Flamigni, *J. Chem. Soc. Faraday Trans.* **1994**, *90*, 2331–2336.

Received: June 28, 2007
Published Online: October 2, 2007

